$\mathbb{Z}_2$ Topological Insulators in Ultracold Atomic Gases

B. Béri and N. R. Cooper

T.C.M. Group, Cavendish Laboratory, J. J. Thomson Avenue, Cambridge CB3 0HE, United Kingdom

We describe how optical dressing can be used to generate band structures for ultracold atoms with nontrivial $\mathbb{Z}_2$ topological order. Time-reversal symmetry is preserved by simple conditions on the optical fields. We first show how to construct optical lattices that give rise to $\mathbb{Z}_2$ topological insulators in two dimensions. We then describe a general method for the construction of three-dimensional $\mathbb{Z}_2$ topological insulators. A central feature of our approach is a new way to understand $\mathbb{Z}_2$ topological insulators starting from the nearly free electron limit.

Recently, it has been realized that the electronic structure of materials is much richer than had previously been thought. The apparently simple band insulator admits an intricate topological classification and can behave as a "topological insulator" which is gapped in the bulk but carries gapless, metallic, states on its surface [1]. The classic example is the integer quantum Hall effect of a two-dimensional (2D) electron system in a magnetic field. In this setting, of 2D with broken time-reversal symmetry (TRS), band insulators are characterized by the integer-valued Chern number [2], which determines the number of metallic surface states. Presently, interest is focused on settings that preserve TRS, since unlike the integer quantum Hall effect, topological insulators are possible in both 2D and 3D. They are classified by a $\mathbb{Z}_2$ invariant [3–5]: Band insulators either are trivial or are nontrivial and support a metallic surface state with interesting spin structure.

While the effects of interactions are rather well understood in the integer quantum Hall effect case, our understanding of strong correlations in $\mathbb{Z}_2$ topological insulators, especially in 3D, is yet in its infancy. Ultracold atomic gases might hold much promise in this direction: They allow the effects of interactions and other perturbations to be explored in a controlled way [6,7]. To take advantage of this in the topological insulator context, it is a crucial prerequisite to find a way to simulate band structures with nontrivial $\mathbb{Z}_2$ invariant. The purpose of this Letter is to solve this problem in both 2D and 3D in a simple, generic, and experimentally feasible fashion.

The standard technique for imposing band structures on ultracold atom gases is the optical lattice: a periodic scalar potential formed from standing waves of light [6]. Optical lattices lead to simple bands with no topological character. In recent work [8], it has been shown that by using the optical fields to couple more than one internal atomic level, leading to effective gauge fields [9], one can generate "optical flux lattices" which break TRS and lead to bands with a nonzero Chern number. Here we show that, by suitable optical dressing, one can form optical lattices that generate non-Abelian gauge fields [7,9], in a way that preserves TRS and leads to bands with nontrivial $\mathbb{Z}_2$ invariant. Our approach is related to methods using optical fields to simulate the effects of spin-orbit coupling [9,10]. It is, however, very different from existing proposed cold-atom implementations of $\mathbb{Z}_2$ topological insulators [11], which imprint non-Abelian gauge potentials on atoms in a deep optical lattice. Our key innovation is to approach the problem from the opposite, nearly free electron limit. This allows for large gaps, with the size set by the recoil energy. Moreover, our proposal can be implemented with a relatively simple laser setup. In addition to its advantages to cold-atom realizations, our nearly free electron approach brings a qualitatively new viewpoint to the field of topological insulators.

We consider an atom with position $\boldsymbol{r}$ and momentum $\boldsymbol{p}$ and with N internal states which is described by the Hamiltonian

$$\hat{H} = \frac{\hat{\boldsymbol{p}}^2}{2m} \mathbb{1}_N + V \hat{M}(\boldsymbol{r}), \tag{1}$$

where V has dimensions of energy. $\mathbb{1}_N$ is the identity, while $\hat{M}(\boldsymbol{r})$ is a position-dependent $N \times N$ matrix acting on the internal states of the atom. To realize a $\mathbb{Z}_2$ topological insulator requires N to be even, owing to a "spin" structure, and the Hamiltonian has to be invariant under time reversal: $\hat{\theta} = i\hat{\sigma}_y \hat{K}$ [1]. (We denote by $\hat{\sigma}_i$ the Pauli matrices in spin space and by $\hat{K}$ complex conjugation.) This requires that $\hat{M} = \hat{\theta}^{-1} \hat{M} \hat{\theta}$. The smallest nontrivial case has $N = 4$ with

$$\hat{M} = \begin{pmatrix} (A+B)\mathbb{1}_2 & C\mathbb{1}_2 - i\hat{\vec{\sigma}} \cdot \vec{D} \\ C\mathbb{1}_2 + i\hat{\vec{\sigma}} \cdot \vec{D} & (A-B)\mathbb{1}_2 \end{pmatrix}. \tag{2}$$

Here A, B, and C are real numbers, and $\vec{D} = (D_x, D_y, D_z)$ is a real three-component vector. $\hat{M}$ can be also written as

$$\hat{M} = A\mathbb{1}_4 + B\hat{\Sigma}_3 + C\hat{\Sigma}_1 + \vec{D}\hat{\Sigma}_2\hat{\vec{\sigma}}, \tag{3}$$

where $\hat{\Sigma}_j$ are the Pauli matrices in the block structure of Eq. (2).

We propose to realize Hamiltonians of this form by using four internal states of an atom, with the entries in Eq. (2) provided by optical fields [9]. Many implementations are possible. In principle, the various transitions between the internal states could be spectrally resolved, allowing the freedom separately to introduce coupling lasers for all transitions (or pairs of lasers for Raman coupling). Our results are very general and could be applied to any such implementation. However, to make the discussion concrete, we shall focus on a particular realization in which the coupling laser operates on a single frequency and therefore has very limited freedom.

The implementation we consider makes use of the properties of the ground state ($^1S_0 = g$) and the long-lived excited state ($^3P_0 = e$) of ytterbium (Yb) or an alkaline earth atom. The usefulness of these two levels for optically induced gauge fields was pointed out by Gerbier and Dalibard [12]: The long lifetime of the excited state reduces spontaneous emission; furthermore, there is a convenient "antimagic" wavelength λ_{am} at which the two states experience scalar optical potentials of opposite signs, allowing state-dependent potentials $\pm V_{am}(r)$ to be implemented. We focus on ^{171}Yb [13], which has nuclear spin $I = 1/2$. Then both g and e have two internal states, and there are four states in total; these will correspond to the 4×4 structure in Eq. (2). We consider the magnetic field to be sufficiently small that the Zeeman splitting is negligible, and all four e-g transitions involve the same frequency $\omega_0 = (E_e - E_g)/\hbar$. Combining the single-photon coupling, with electric field $\vec{E} = \vec{\mathcal{E}}e^{-i\omega t} + \vec{\mathcal{E}}^* e^{i\omega t}$, with the state-dependent potential V_{am} leads to the optical potential which in the rotating wave approximation [14] is

$$V\hat{M} = \begin{pmatrix} \left(\frac{\hbar}{2}\Delta + V_{am}\right)\mathbb{1}_2 & -i\hat{\vec{\sigma}} \cdot \vec{\mathcal{E}}d_r \\ i\hat{\vec{\sigma}} \cdot \vec{\mathcal{E}}^* d_r & -\left(\frac{\hbar}{2}\Delta + V_{am}\right)\mathbb{1}_2 \end{pmatrix}, \quad (4)$$

where $\Delta = \omega - \omega_0$ is the detuning. The form of the off-diagonal term follows from the Wigner-Eckardt theorem, with d_r the reduced dipole moment [15]. A comparison of Eq. (4) with Eq. (2) shows that the optical coupling (4) describes a TRS situation provided all components of $\vec{\mathcal{E}}$ have the same phase, in which case $\vec{\mathcal{E}}$ can be chosen real.

Two-dimensional systems.—We consider first cases in which the atoms are tightly confined in the z direction, so their motion in the x-y plane is (quasi-)two-dimensional. A $\mathbb{Z}_2$ topological insulator can be formed by choosing the electric field, detuning, and state-dependent potential in Eq. (4) such that

$$d_r\vec{\mathcal{E}} = V[\delta, \cos(r \cdot \kappa_1), \cos(r \cdot \kappa_2)], \quad (5)$$

$$\frac{\hbar}{2}\Delta + V_{am}(r) = V\cos[r \cdot (\kappa_1 + \kappa_2)] \quad (6)$$

with $\kappa_1 = (1, 0, 0)\kappa$ and $\kappa_2 = (\cos\theta, \sin\theta, 0)\kappa$. The amplitudes are chosen to have a common energy scale V, which can be interpreted as a measure of the Rabi coupling. This energy scale should be compared to the characteristic kinetic energy scale, the recoil energy $E_R \equiv \hbar^2\kappa^2/2m$. The interspecies coupling (5) is formed from three (standing) waves of linearly polarized light at the coupling frequency ω: two of equal amplitude with wave vectors in the 2D plane (κ_1 for y polarization and κ_2 for z polarization) and one with a wave vector normal to the 2D plane for x polarization with an amplitude smaller by a factor of δ. Since $\omega \simeq \omega_0$, the magnitude of the in-plane wave vectors is $\kappa \simeq 2\pi/\lambda_0$ with $\lambda_0 = 578$ nm the wavelength of the e-g transition. The spatial dependence of V_{am} is set by a standing wave at the antimagic wavelength λ_{am} [12], which creates a state-dependent potential with $|\kappa_1 + \kappa_2| = 4\pi/\lambda_{am}$. This fixes the angle $\theta = 2\arccos(\pm\lambda_0/\lambda_{am})$. For Yb, $\lambda_0/\lambda_{am} \simeq 1/2$ (to an accuracy of about 3%), so $\theta \simeq \pm 2\pi/3$. For simplicity, in all following discussions we fix $\theta = 2\pi/3$ and define $a \equiv 4\pi/(\sqrt{3}\kappa)$. The optical coupling $\hat{M}$ then has the symmetry of a triangular lattice with lattice vectors $a_1 = (\sqrt{3}/2, -1/2)a$ and $a_2 = (0, 1)a$.

The physics arising from this form of optical coupling is most clearly exposed by applying a unitary transformation $\hat{U} = 2^{-1/2}(\mathbb{1}_4 - i\hat{\Sigma}_3\hat{\sigma}_2)$ [16] to the dimensionless coupling $\hat{M}$:

$$\hat{M}' = \hat{U}^\dagger \hat{M}\hat{U} = c_1\hat{\Sigma}_1 + c_2\hat{\Sigma}_2\hat{\sigma}_3 + c_{12}\hat{\Sigma}_3 + \delta\hat{\Sigma}_2\hat{\sigma}_1. \quad (7)$$

We have used the shorthand $c_i \equiv \cos r \cdot \kappa_i$ and $c_{12} \equiv \cos[r \cdot (\kappa_1 + \kappa_2)]$. For $\delta = 0$ this matrix decouples into two 2×2 blocks, one for each eigenvalue of $\hat{\sigma}_3$, as does the Hamiltonian since the kinetic energy (1) is diagonal. Thus, the four-level system decouples into two two-level subsystems, each experiencing its own form of optical dressing, $c_1\hat{\Sigma}_1 \pm c_2\hat{\Sigma}_2 + c_{12}\hat{\Sigma}_3$, differing only in the sign of the c_2 term. This is precisely the optical dressing required to realize the "triangular" optical flux lattice described in Ref. [8] (see [17]). This optical flux lattice causes the atoms to experience a (periodic) effective magnetic field with $N_\phi = 2$ flux quanta in the unit cell. For $V \gtrsim 0.2E_R$ the lowest energy band (which is twofold degenerate [8]) is separated in energy from higher bands. This band is topologically nontrivial, having a Chern number of ± 1, with the sign set by the net sign of the coefficients c_1, c_2, and c_{12}. Since this sign differs for the two subsystems, their lowest bands have equal and opposite Chern numbers. (This is required by the fact that these subsystems are related by time reversal.) Thus, for $\delta = 0$ the optical dressing realizes the band structure required to generate the quantum spin Hall (QSH) effect: There are two decoupled subsystems, the lowest energy bands of which have Chern numbers ± 1. Each of these bands is

filled when the 2D density of fermions (in that component) is equal to the magnetic flux density: $N_\phi/(\sqrt{3}/2a^2) = 4/(\sqrt{3}a^2)$. When both bands are filled, at a total fermion density of $n_{2D} = 8/\sqrt{3}a^2$, the bulk of the system is gapped. However, there will be a metallic surface state involving counterpropagating edge modes of opposite spin. This metallic surface state is the hallmark of the topological order that characterizes the QSH effect.

The QSH effect is a special case of the $\mathbb{Z}_2$ topological insulator. The $\mathbb{Z}_2$ topological insulator, in general, does not allow separation into two decoupled systems but retains counterpropagating edge states that are protected only by TRS. A nonzero value of δ introduces a coupling between the two spin states in a manner that preserves TRS, in direct analogy to the effects of spin-orbit coupling on the electronic structure of solids. In Fig. 1, we show the few lowest energy bands for a small nonzero value of δ. (The bands were calculated by numerical diagonalization in the plane wave basis.) For $\delta = 0$ all bands are fourfold degenerate. For $\delta \neq 0$ this degeneracy splits into two doubly degenerate branches at most wave vectors. However, the fourfold degeneracy remains at three nonequivalent symmetry points in k space: $\boldsymbol{\kappa}_1/2$, $\boldsymbol{\kappa}_2/2$, and $(\boldsymbol{\kappa}_1 + \boldsymbol{\kappa}_2)/2$. (The reciprocal lattice vectors are simply given by $\boldsymbol{\kappa}_i$.)

Because of the coupling between the two subsystems, the Chern number of a subsystem is no longer well defined, but the bands still carry a topological character since the $\delta = 0$ case is adiabatically connected to the QSH limit. To demonstrate this, one has to use a more general $\mathbb{Z}_2$ invariant [18]. This invariant takes a particularly simple form for our system owing to its symmetry under spatial inversion, $\hat{P}: \boldsymbol{r} \rightarrow -\boldsymbol{r}$. Inversion symmetric insulators, as shown by Fu and Kane [18,19], are $\mathbb{Z}_2$ nontrivial if

$$\prod_{n,m=0,1} \prod_{\alpha \in \text{filled}} \xi_{nm}^{(\alpha)} = -1, \qquad (8)$$

where $\xi_{nm}^{(\alpha)}$ are the inversion eigenvalues corresponding to the αth Kramers doublet of bands at the momenta $\boldsymbol{\Gamma}_{nm} = (n\boldsymbol{\kappa}_1 + m\boldsymbol{\kappa}_2)/2$ ($n, m = 0, 1$). Evaluating Eq. (8) for our system, we find that it is indeed in a topological phase: The points with fourfold degeneracies contribute with (-1), while $\boldsymbol{k} = 0$ contributes with unity, as indicated in Fig. 1. Although we have shown bands for the special case of a triangular lattice, our approach is very general: Starting from an optical flux lattice of any symmetry [8], our method will lead to a 2D $\mathbb{Z}_2$ topological insulator.

Three-dimensional systems.—Our approach has the remarkable feature that it generalizes naturally to 3D topological insulators. One simply needs to substitute

$$c_{12} \rightarrow c_{12} + \delta(\mu + c_{13} + c_{23}), \qquad \delta \rightarrow \delta \cos(\boldsymbol{\kappa}_3 \cdot \boldsymbol{r}), \qquad (9)$$

where our notation follows that of Eq. (7), and we use $\boldsymbol{\kappa}_3 = (0, 0, 1)\kappa$. That this system is a good candidate for a topological insulator can be checked by using the parities as in Eq. (8), but the product is now over eight momenta: $\boldsymbol{\Gamma}_{nml} = (n\boldsymbol{\kappa}_1 + m\boldsymbol{\kappa}_2 + l\boldsymbol{\kappa}_3)/2$ ($n, m, l = 0, 1$) [18]. Evaluating the product shows that the parities are those of a $\mathbb{Z}_2$ topological phase for a large range of parameters. Importantly, this range includes systems which are insulators as well. This is demonstrated in Fig. 2, where we show the few lowest energy bands of the model for a point in the regime where the parity product is negative. A clear band gap separates the lowest four bands from the higher bands, showing that the system is an insulator. This extension to 3D entails additional geometrical constraints on the wave vectors of the coupling and state-dependent lasers. For example, for $\boldsymbol{\kappa}_i \perp \boldsymbol{\kappa}_j$ the state-dependent potential c_{ij} has to have periodicity $\lambda_0/\sqrt{2}$. For Yb, this differs from that achieved by the antimagic wavelength $\lambda_{\text{am}}/2 \simeq \lambda_0$, so
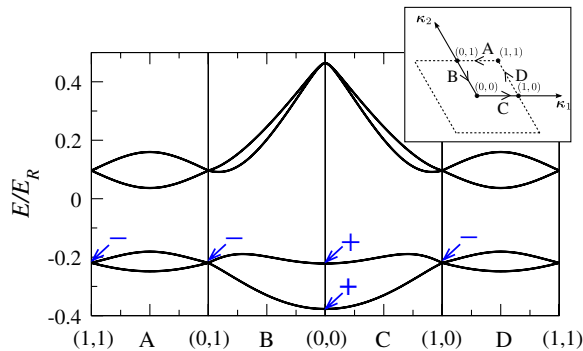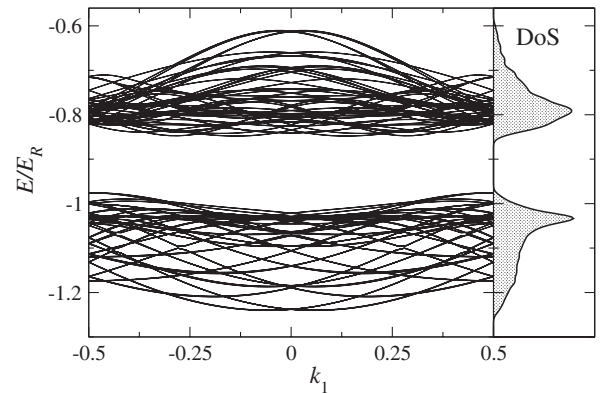

FIG. 1 (color online). Lowest energy bands for the 2D topological insulator with $V = 0.5E_R$ and $\delta = 0.25$ for wave vectors on the perimeter of the parallelogram (shown in the inset) with corners $\boldsymbol{\Gamma}_{nm} = (n\boldsymbol{\kappa}_1 + m\boldsymbol{\kappa}_2)/2$ ($n, m = 0, 1$). Each band is twofold degenerate, with fourfold degeneracies at $\boldsymbol{\Gamma}_{nm} \neq 0$. The four bands with $E/E_R \lesssim -0.1$ have nontrivial $\mathbb{Z}_2$ invariant, as follows from the eigenstate parities ($\pm$) at $\boldsymbol{\Gamma}_{nm}$.

FIG. 2. Lowest energy bands for the model Eq. (9), for a set of wave vectors $\boldsymbol{k} = \sum_i k_i \boldsymbol{\kappa}_i$ with k_2 and k_3 uniformly spaced across the Brillouin zone. The parameters are $V = 0.9E_R$, $\delta = 1.0$, and $\mu = -0.2$. The four bands with $E/E_R \lesssim -0.9$ have nontrivial $\mathbb{Z}_2$ invariant which, together with the clear band gap, demonstrates the topological insulator phase. The right-hand panel shows the density of states.

in this case there will be an additional state-independent potential [12]. We have checked that this does not affect the appearance of the $\mathbb{Z}_2$ topological insulator phase for the lowest 4 bands.

While the robust and simple realization of a 3D topological insulator is a key result, the choice (9) might seem fortuitous. The remaining part of this Letter introduces a constructive approach for finding 3D systems with $\mathbb{Z}_2$ nontrivial parities. A hint for this is given by the 2D case, if one notes that the Γ_{nm} with negative parities are precisely the points in momentum space with fourfold degeneracies. This can be understood by using the following symmetry considerations. The Hamiltonian is invariant under translations by the lattice vectors a_i. The associated reciprocal lattice vectors are simply κ_j and define the Brillouin zone for the conserved momentum k. By using the Bloch decomposition $\psi_k = \exp(i k \cdot r) u_k(r)$, the eigenvalue problem at each k point follows from the Hamiltonian

$$\hat{H}_{\mathbf{k}} = \frac{(\hat{p} + \hbar k)^2}{2m} \mathbb{1}_N + V \hat{M}'(r) \qquad (10)$$

acting on lattice periodic functions. $\hat{H}_k$ has half-translation symmetries $\hat{T}_1 = \hat{\Sigma}_2 \hat{T}_{a_1/2}$ and $\hat{T}_2 = \hat{\Sigma}_1 \hat{\sigma}_3 \hat{T}_{a_2/2}$. (Here $\hat{T}_{\mathbf{v}}$ is the operator of translation with the vector $\mathbf{v}$.) At the special momenta Γ_{nm}, $\hat{H}_{\Gamma_{nm}}$ is invariant under both generalized time-reversal and inversion operators: $\hat{\theta}_{nm} = \exp(-i 2 \Gamma_{nm} \cdot r) \hat{\theta}$ and $\hat{P}_{nm} = \exp(-i 2 \Gamma_{nm} \cdot r) \hat{P}$. The two symmetries commute; hence, $u_{\Gamma_{nm}}$ and its Kramers partner $\hat{\theta}_{nm} u_{\Gamma_{nm}}$ share the same inversion eigenvalue ξ_{nm}. From the fact that $\hat{T}_i^2 = 1$ on lattice periodic functions, it follows that $\hat{T}_i \hat{P}_{nm} = \exp(-i \Gamma_{nm} \cdot a_i) \hat{P}_{nm} \hat{T}_i$. This means that at Γ_{10} the application of $\hat{T}_1$, at Γ_{01} of $\hat{T}_2$, and at Γ_{11} of either $\hat{T}_i$ reverses the inversion eigenvalue: This requires, first, that the energies are fourfold degenerate and, second, that for each energy the inversion eigenvalues come in opposite pairs [20]. This explains why the degenerate points contributed with (-1) in Eq. (8).

These considerations allow one to construct 3D configurations with $\mathbb{Z}_2$ nontrivial parities: Consider a model which has a reflection symmetry $a_1 \leftrightarrow a_2$ and a half-translation symmetry by $d = \frac{1}{2}(a_1 + a_2 + a_3)$. ($a_3$ is the third primitive lattice vector.) The reflection symmetry results in $\xi_{nm1} = \xi_{mn1}$, while the half-translation symmetry means that at Γ_{001} and Γ_{111} the inversion eigenvalues come in opposite pairs for each energy, making the energies fourfold degenerate. Thus, for any $2N$ doublets we have $\prod_{\alpha=1}^{2N} \prod_{nm} \xi_{nm1}^{(\alpha)} = 1$, so the net parity is $\prod_{\alpha=1}^{2N} \prod_{nm} \xi_{nm0}^{(\alpha)}$. Assume that the model can be written as $\hat{H}_k = \hat{H}_k^{(2D)} + \frac{(\hat{p} + \hbar k)_z^2}{2m} + \hat{H}_k^{(pert)}$. If $\hat{H}_k^{(2D)}$ realizes a two-dimensional topological insulator with $2N$ filled Kramers pair of bands, then $\prod_{\alpha=1}^{2N} \prod_{nm} \xi_{nm0}^{(\alpha)} = -1$ for a weak $\hat{H}_k^{(pert)}$. This means that the net parity for the lowest $2N$ Kramers pairs must be

negative: The model is *guaranteed* to have the parities of a 3D $\mathbb{Z}_2$ topological insulator. The choice Eq. (9) is one of the simplest ones consistent with this strategy.

In summary, we have described how simple forms of optical coupling can lead to low-energy bands that have nontrivial $\mathbb{Z}_2$ topological invariant, in both 2D and 3D. Weakly interacting fermions filling these bands will form incompressible band insulators and exhibit the expected features of these topological phases: notably, the metallic surface states. The properties of these surface states could be probed by studying the (spin-resolved) collective modes of the atomic gas. Since we work close to the nearly free electron limit, the required temperature scale is set by the recoil energy, which is of the order of 0.1 mK in the case of ^{171}Yb, easily accessible in experiments.

The realization of these topological band structures in ultracold atomic gases will allow the study of interesting properties that cannot readily be explored in solid state systems. An important issue concerns the effects of (attractive or repulsive) interactions [21]. Weak interactions can affect the properties of the surface modes, while strong interactions may drive the system into strongly correlated topological phases, either with TRS preserved [22] or with broken TRS in which case they are related to fractional quantum Hall states. Furthermore, cold-atom implementations will allow studies of the effects of tuning the nature of the bands, inducing transitions in their topology. Introducing a phase difference between the electric fields in (4) breaks TRS; this could be used to study quantum phase transitions out of the $\mathbb{Z}_2$ topological insulator phase, into (for example) integer quantum Hall states.

[1] M. Z. Hasan and C. L. Kane, Rev. Mod. Phys. **82**, 3045 (2010); X.-L. Qi and S.-C. Zhang, arXiv:1008.2026.

[2] D. J. Thouless, M. Kohmoto, M. P. Nightingale, and M. den Nijs, Phys. Rev. Lett. **49**, 405 (1982).

[3] C. L. Kane and E. J. Mele, Phys. Rev. Lett. **95**, 146802 (2005); L. Fu, C. L. Kane, and E. J. Mele, Phys. Rev. Lett. **98**, 106803 (2007).

[4] J. E. Moore and L. Balents, Phys. Rev. B **75**, 121306 (2007).

[5] R. Roy, Phys. Rev. B **79**, 195321 (2009); **79**, 195322 (2009).

[6] I. Bloch, J. Dalibard, and W. Zwerger, Rev. Mod. Phys. **80**, 885 (2008).

[7] M. Lewenstein et al., Adv. Phys. **56**, 243 (2007).

[8] N. R. Cooper, Phys. Rev. Lett. **106**, 175301 (2011).

[9] J. Dalibard, F. Gerbier, G. Juzeliūnas, and P. Öhberg, arXiv:1008.5378 [Rev. Mod. Phys. (to be published)].

[10] A. M. Dudarev, R. B. Diener, I. Carusotto, and Q. Niu, Phys. Rev. Lett. **92**, 153005 (2004); T. D. Stanescu, C. Zhang, and V. Galitski, Phys. Rev. Lett. **99**, 110403 (2007); Y.-J. Lin, K. Jimenez-Garcia, and I. B. Spielman, Nature (London) **471**, 83 (2011).

[11] N. Goldman *et al.*, Phys. Rev. Lett. **105**, 255302 (2010); A. Bermudez *et al.*, Phys. Rev. Lett. **105**, 190404 (2010).

[12] F. Gerbier and J. Dalibard, New J. Phys. **12**, 033007 (2010).

[13] S. Taie *et al.*, Phys. Rev. Lett. **105**, 190401 (2010).

[14] C. Cohen-Tannoudji, J. Dupont-Roc, and G. Grynberg, *Atom-Photon Interactions* (Wiley, New York, 1992).

[15] L. D. Landau and E. M. Lifshitz, *Quantum Mechanics* (Pergamon, London, 1958).

[16] The time-reversal operator $\hat{\theta}$ is invariant under $\hat{U}$.

[17] Note that κ_2 of Ref. [8] is $\kappa_1 + \kappa_2$ in the notation here.

[18] L. Fu and C. L. Kane, Phys. Rev. B **76**, 045302 (2007).

[19] See Supplemental Material at http://link.aps.org/supplemental/10.1103/PhysRevLett.107.145301 for additional background information on the Fu-Kane formula for the $\mathbb{Z}_2$ invariant.

[20] At $\boldsymbol{\Gamma}_{00}$ the fourfold degeneracy is split into two doublets; these two doublets can have the same or different inversion eigenvalues.

[21] To study interaction effects, it may help to use an implementation based on hyperfine levels, for which collisional losses can be reduced.

[22] Z. Wang, X.-L. Qi, and S.-C. Zhang, Phys. Rev. Lett. **105**, 256803 (2010).